Environmental Pollution 316 (2023) 120501

Contents lists available at ScienceDirect

Environmental Pollution

journal homepage: www.elsevier.com/locate/envpol

Characterization of columnar aerosol over a background site in Central Asia☆

Dipesh Rupakheti [a,i,*], Maheswar Rupakheti [b], Mukesh Rai [c], Xingna Yu [e], Xiufeng Yin [d], Shichang Kang [d,f], Musapar D. Orozaliev [g], Valery P. Sinyakov [g], Sabur F. Abdullaev [h], Ishaq Dimeji Sulaymon [a], Jianlin Hu [a]

[a] Jiangsu Key Laboratory of Atmospheric Environment Monitoring and Pollution Control, Collaborative Innovation Center of Atmospheric Environment and Equipment Technology, School of Environmental Science and Engineering, Nanjing University of Information Science and Technology, Nanjing, 210044, China
[b] Institute for Advanced Sustainability Studies, Potsdam, Germany
[c] International Centre for Integrated Mountain Development, Lalitpur, Nepal
[d] State Key Laboratory of Cryospheric Science, Northwest Institute of Eco-Environment and Resources, Chinese Academy of Sciences, Lanzhou 730000, China
[e] Key Laboratory for Aerosol-Cloud-Precipitation of China Meteorological Administration, Collaborative Innovation Center on Forecast and Evaluation of Meteorological Disasters, Nanjing University of Information Science and Technology, Nanjing 210044, China
[f] University of Chinese Academy of Sciences (UCAS), Beijing 100049, China
[g] Institute of Innovative Professions, Kyrgyz State University of Construction, Transport and Architecture Named After N Isanov, Bishkek, Kyrgyzstan
[h] Physical Technical Institute of the Academy of Sciences of Tajikistan, Dushanbe, Tajikistan
[i] Institute of Fundamental Research and Studies, Kathmandu 44600, Nepal

ARTICLE INFO

Keywords:
Aerosol optical depth
Ångström exponent
Heavy aerosol events
Issyk-Kul
Central Asia
AERONET

ABSTRACT

Ground-based observational characterization of atmosphere aerosols over Central Asia is very limited. This study investigated the columnar aerosol characteristics over Issyk-Kul, Kyrgyzstan, a background site in Central Asia using the long-term (~14 years: August 2007–November 2021) data acquired with the Cimel sunphotometer. The mean aerosol optical depth (AOD) and Ångström exponent (AE) during the observation period were 0.14 ± 0.10 and 1.19 ± 0.41, respectively. Both AOD and AE varied across seasons, with highest AOD in spring (0.17 ± 0.17). Regarding the aerosol types, clean continental aerosols were dominant type (65%), followed by mixed aerosols (~19%), clean marine aerosols (~14%), dust (0.8%), and urban/industrial and biomass burning aerosol (0.7%). The aerosol volume size distribution was bimodal indicating the influence of both anthropogenic and natural aerosols with clear dominance of coarse mode during the spring season. Mainly dust and mixed aerosols were present during high aerosol episodes while the coarse mode aerosol volume concentration was 7.5 (strong episodes) and ~19 (extreme episodes) times higher than the whole period average. Aerosol over this background sites were from local and regional sources with some contribution of long-range transport.

1. Introduction

Atmospheric aerosols from both anthropogenic activities and natural sources, being an important constituent of the atmosphere, plays significant roles in altering the earth's radiative balance, influencing hydrological and cryosphere systems, degrading air quality, and adversely impacting human health and agriculture productivity (Chameides et al., 1999; Rosenfeld, 2000; Ramanathan et al., 2001; Kampa and Castanas, 2008; Burney and Ramanathan, 2014; Cohen et al., 2017; Hu et al., 2017; Kang et al., 2019; Liu et al., 2020; Wang et al., 2021). There are still large uncertainties understanding and quantifying the role of aerosols on climate system, among others, largely because of insufficient knowledge on aerosol morphology, chemical characteristics and distributions, magnitudes and trends, especially over intense aerosol source regions across the globe, in particular Asia (Kaufman et al., 2002; Srivastava et al., 2011; Stocker et al., 2013; IPCC, 2021; Ramachandran

☆ This paper has been recommended for acceptance by Pavlos Kassomenos.

* Corresponding author. Jiangsu Key Laboratory of Atmospheric Environment Monitoring and Pollution Control, Collaborative Innovation Center of Atmospheric Environment and Equipment Technology, School of Environmental Science and Engineering, Nanjing University of Information Science and Technology, Nanjing, 210044, China.
E-mail addresses: dipesh.rupakheti@nuist.edu.cn, drupakheti2@gmail.com (D. Rupakheti).

https://doi.org/10.1016/j.envpol.2022.120501
Received 10 June 2022; Received in revised form 1 October 2022; Accepted 19 October 2022
Available online 22 October 2022

and Rupakheti, 2022).

Central Asia is situated almost in the middle of the global dust belt that extends from northern Africa and passes through deserts in the Arabian region and Taklamakan Desert up to the Gobi Desert (Hofer et al., 2017). The Taklamakan, Kara-Kum and Kyzyl-Kum deserts, as well as the Aral Sea region are important and major dust source region for Central Asia and rest of the Northern Hemisphere (Prospero et al., 2002; Chen et al., 2013a). The strong south-westerly winds low-pressure system over western Siberia facilitate development of dust storms that transport dust from deserts in northern Africa and Arabian Peninsula towards Central Asia (Liu et al., 2019), resulting in the occurrence of numerous dust episodes during summer and autumn season (Golitsyn and Gillette, 1993). Climate change, over-exploitation of the water resources, population growth, inappropriate land management are some of the important factors of environmental deterioration resulting in to desertification, biodiversity loss, soil salinization and frequent sand storms in the Central Asian region (Yu et al., 2019 and references therein). On the other hand, Central Asia lies in proximity of the Tian-shan Mountain, the Pamirs, the Himalayas and Tibetan Plateau region, which are considered as 'the water tower of Asia' for housing large glaciers that feed major Asian rivers which sustain the life of more than a billion population (Immerzeel et al., 2010). Anthropogenic pollution and dust from the Central Asia region transported to the glaciers over those mountain ranges influence atmospheric radiative forcing through heating the atmosphere and altering the surface albedo of the glaciers and snowfields (Kang et al., 2019; Sierra-Hernández et al., 2019; Hu et al., 2022). Hence, analysis of atmospheric pollution over this vast region is one of the preliminary steps in understanding what gets transported towards the Himalayas, Tibetan Plateau and beyond.

Central Asia mainly covers five countries viz. Kazakhstan, Kyrgyzstan, Tajikistan, Uzbekistan and Turkmenistan. An overview of previous studies on atmospheric pollution over Central Asia have already been presented in recent studies (Hofer et al., 2017; Rupakheti et al., 2019, 2020); thus, here we will mention the relevant studies over Kyrgyzstan only. Using a handheld sunphotometer in Issyk-Kul Lake, Semenov et al. (2005) studied the aerosol optical depth (AOD), columnar Angstrom exponent (AE) and water vapor, and their interrelationships. Chen et al. (2013b) examined the relationship between AOD and particulate matter (PM) concentrations, where a high correlation was reported, especially during the spring and autumn period due to the dust storms. Chen et al. (2013a) investigated the vertical distribution of dust and identified the Taklimakan Desert and the Aral Sea basin as regional dust source and the deserts of the Middle East region as long-range transport sources. However, Dewan et al. (2015), using stable isotopes of strontium to investigate the sources of airborne PM in Kyrgyzstan, stated that the Aral Sea sediments have very minimal effect on the air quality of Kyrgyzstan. Sizov et al. (2015) investigated the trend in AOD over the Issyk-Kul region during 1984–2009 and reported the increase in AOD during recent years. Recently, Rupakheti et al. (2019) utilized the satellite AOD data over the whole of Central Asia and reported the lowest AOD over Kyrgyzstan as compared with the other four countries in the region. In addition to using ground and satellite-based datasets to study the atmospheric pollution over this region, some studies have utilized other environmental media like soil and sediments to report the pollution. Li et al. (2020) have analyzed polycyclic aromatic hydrocarbons (PAHs), total organic carbon (TOC) and n-alkanes in the soil surrounding two lakes, Issyk-Kul and Son-Kul from Kyrgyzstan . Rupakheti et al. (2021) have reported the Black carbon (BC, an important contributor to global warming) in the soil from three central Asian countries, including Kyrgyzstan. Monitoring atmospheric pollution in Central Asia can provide valuable information on the regional source of pollutants and on characteristics of pollution transport which will be beneficial for the validation of the atmospheric models (Chen et al., 2013c), besides advancing understanding their impacts in the downwind mountain regions with sensitive ecosystems.

This study has been designed keeping in mind the lack of recent studies to explain the magnitude of aerosol loading and other associated aerosol properties over Central Asia. We have utilized the data acquired with a Cimel sunphotometer installed under the NASA AERONET (AErosol Robotic NETwork) project over a long period from August 2007–November 2021 to understand the aerosol loading, aerosol types and size distribution of the aerosol over a background site, Issyk-Kul Lake in Kyrgyzstan. We also classified the aerosol based on different parameters and further investigated the 'heavy aerosol' events. The Hybrid Single-Particle Lagrangian Integrated Trajectory (HYSPLIT) model along with potential source contribution function (PSCF) has been conducted to understand the source of aerosol.

2. Materials and methods

2.1. Monitoring site

Kyrgyzstan, situated between 39 and 44 °N latitude and 69–81 °E longitude, is among the five countries in the central Asia region, with a total area of about 200 thousand km^2 and an estimated population of about 6.5 million. The country shares its border with Kazakhstan (north), China (east), Tajikistan (south) and Uzbekistan (west). Issyk-Kul station is situated in the shoreline of the Issyk-Kul Lake (42.6 °N, 77.0 °E, 1650 m asl), a closed-basin lake with a catchment area of ~22,000 km^2. It is the seventh deepest and the tenth largest lake in the world. The Issyk-Kul Lake with more than 6200 km^2 area is surrounded by two giant mountain ranges viz. Kungey Ala-Too (towards north) and Terskey Ala-Too (towards south), creating a complex geophysical setting (Fig. 1) that hinders the transport of polluted air mass from the nearby big cities like Bishkek City (the capital city of Kyrgyzstan) and Almaty (huge industrial center and previous capital of Kazakhstan) (Semenov et al., 2005). Without any local industrial activities and being located away from major cities, the atmosphere over the Issyk-Kul basin can be considered as the background, typical for rural conditions of the central Asia mountainous region (Semenov et al., 2005; Sizov et al., 2015).

2.2. AERONET instrumentation and data

The NASA AERONET program (https://aeronet.gsfc.nasa.gov/) installed a CIMEL sun-photometer in Issyk Kul in August 2007 to understand the columnar aerosol properties over a central Asian background atmosphere. The sun-photometer measures the direct-sun irradiance at eight channels between 340 and 1020 nm and sky radiance at four channels between 440 and 1020 nm (Holben et al., 2001a, 2001b, 1998). The AERONET website reports aerosol data in three different level of processing: level 1 (unscreened data), level 1.5 (cloud screened data) and level 2.0 (quality-assured data). In this study, we retrieved the Level 2 version 3 data (cloud screened and quality assured) (Giles et al., 2019; Smirnov et al., 2000) collected during August 2007–November 2021, which consist of 3021 days of high-quality data. AERONET datasets possess low measurement uncertainties as compared to satellite datasets (Sinyuk et al., 2020; Sayer et al., 2012). The AERONET instruments are routinely calibrated approximately every 6–12 months following an elaborate procedure (Dubovik et al., 2002; Holben et al., 2001a, 2001b) to ensure continuity and measurement quality. The uncertainties in AOD (direct sun) is less than ± 0.01 for wavelengths >0.44 μm and is less than ± 0.02 for shorter wavelengths (Holben et al., 2001a, 2001b). AOD, fine mode fraction (FMF, i.e., contribution of fine-mode AOD on total AOD), Ångström exponent (AE) and volume size distribution (VSD) data were retrieved for this study. Other parameters like single scattering albedo (SSA), asymmetry parameter (ASY), and refractive index (RI) were not utilized as they pose high uncertainty at low aerosol loading condition (AOD <0.4) (Dubovik et al., 2000). More details on the AERONET observations, data processing and related uncertainties are provided in earlier literature (Smirnov et al., 2000; Holben et al., 2001a, 2001b). Three parameters analyzed in this study provided with the results that can still be considered valuable as the

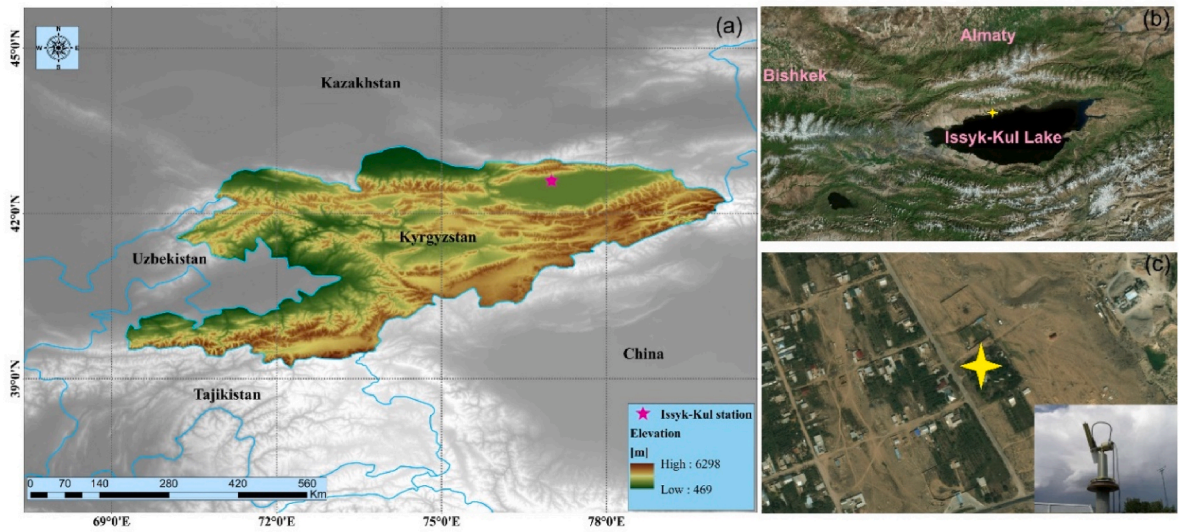

Fig. 1. The location of Issyk-Kul AERONET station (pink star) in Kyrgyzstan (a), satellite image of the Issyk-Kul Lake and its surroundings (b) and satellite image of Issyk-Kul station and its surrounding (c). A CIMEL sunphotometer in action in the inset of (c) is obtained from the AERONET website (https://aeronet.gsfc.nasa.gov/). The satellite images used in (b) and (c) were obtained from Bing Maps (www.bing.com/maps). (For interpretation of the references to colour in this figure legend, the reader is referred to the Web version of this article.)

stations to measure long-term columnar aerosol properties over this vast landmass, in particular at the background conditions, are very scarce.

3. Results and discussions

3.1. Overview on AOD and AE: frequency and temporal variation

During the whole observation period (August 2007–November 2021), the median (mean ± standard deviation) AOD, AE, and FMF were found to be 0.11 (0.14 ± 0.10), 1.22 (1.19 ± 0.41) and 0.68 (0.67 ± 0.19), respectively. Due to the several aerosol events or episodes (explained in Section 3.4), the median values were lower than the mean AOD (Pokharel et al., 2019). For the same period, their daily mean values ranged between 0.01 –1.47 (AOD), 0.02–2.43 (AE) and 0.15–1.00 (FMF), which indicated wide variations in aerosol loading with presence of different aerosol types (detail in Section 3.2). The frequency distribution of daily AOD and AE across seasons has been presented in Fig. 2. Both AOD and AE exhibited unimodal distribution with modal AOD at ca. 0.15 and AE at ca. 1.2. About 96% of the sampling days (2897 days) were 'clean' days as the condition with anthropogenic AOD higher than 0.3 is considered a polluted atmosphere or pollution hotspot (Ramanathan et al., 2007). Though it is not possible here to separate how much of AOD was contributed by the anthropogenic emissions, AOD higher than 0.3 was observed only on 124 days (out of 3021 days of available L2 data), mostly during dust storms in spring and summer. A previous study conducted over Central Asia using the satellite retrieved data reported a similar result for Kyrgyzstan (~97% of the days during 2002–2017 were clean days) (Rupakheti et al., 2019). The AE data was spread over a wide range indicating the presence of aerosol from various sources as the higher AE indicates presence of fine particles (sourced from anthropogenic activities like biomass burning and fossil fuel combustion), and lower AE indicates coarse particles (sourced from natural sources like dust) (Holben et al., 2001a, 2001b; Schuster et al., 2006).

The AOD and AE data has been compared with multiple sites across the region (Table 1) to understand the situation over the Issyk-Kul. Although the observations by these studies are not made in the same period, it however provides some useful insights for the scientific community to understand the aerosol properties and potential sources over the less-studied Central Asian region. A study based on the same site utilizing the data collected for 25 years (1985–2009) using the filter

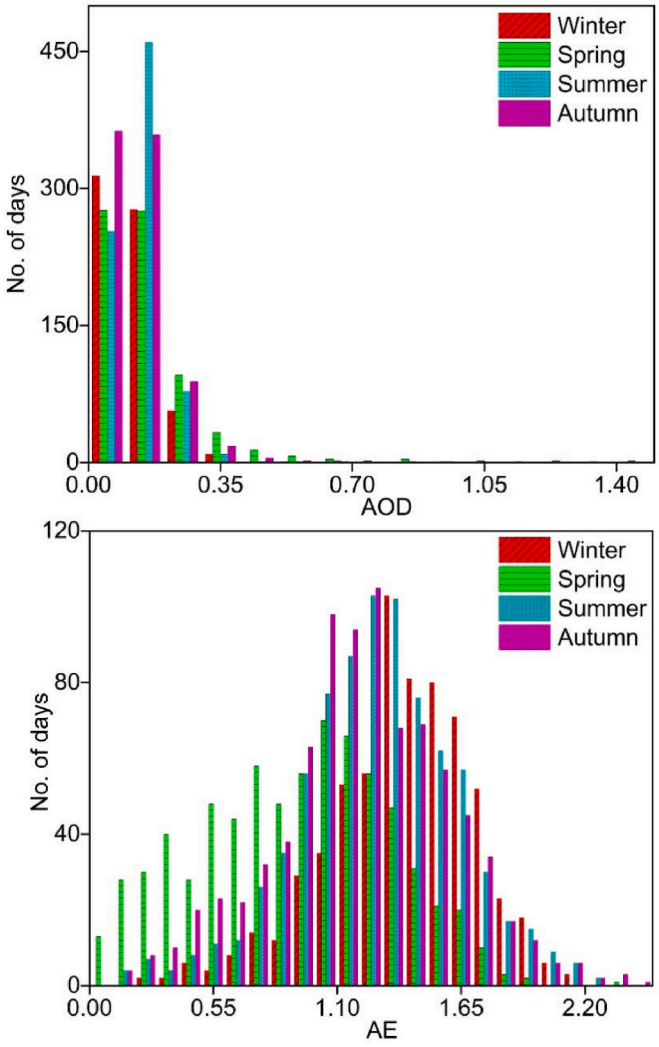

Fig. 2. Frequency distribution of seasonal AOD and AE.

Table 1
Comparison of AOD and AE observed in Issyk-Kul with other sites.

Sites	Duration	AOD	AE	References
Issyk-Kul, Kyrgyzstan	2007–2021	0.14 ± 0.10	1.19 ± 0.41	***This study***
	Winter	0.12 ± 0.06	1.39 ± 0.32	
	Spring	0.17 ± 0.17	0.91 ± 0.43	
	Summer	0.13 ± 0.07	1.27 ± 0.36	
	Autumn	0.12 ± 0.08	1.22 ± 0.38	
Issyk-Kul, Kyrgyzstan	2000–2004	0.10 ± 0.03	1.25 ± 0.36	Semenov et al. (2005)
Issyk-Kul, Kyrgyzstan	1984–2009	0.128 ± 0.03	–	Sizov et al. (2015)
Kyrgyzstan	2002–2017	0.11 ± 0.13	1.41 ± 0.13	Rupakheti et al. (2019)
Dushanbe, Tajikistan	2010–2018	0.28 ± 0.20	0.82 ± 0.40	Rupakheti et al. (2020)
Muztagh Ata, Eastern Pamirs	2011	0.14 ± 0.07	0.70 ± 0.27	Yan et al. (2015)
Mt. Waliguan, China	2009–2010	0.14 ± 0.07	0.59 ± 0.24	Che et al. (2011)
Dunhuang, China	1999–2000	0.14–0.37	0.01–0.66	Xia et al. (2004)
Zanjan, Iran	2006–2008	0.28 ± 0.14	0.73 ± 0.30	Bayat et al. (2011)
Nam Co, TP	2006–2016	0.045 ± 0.047	–	Pokharel et al. (2019)
QOMS, TP	2009–2017	0.043 ± 0.039	–	Pokharel et al. (2019)
Lahore, Pakistan	2001–2018	0.81 ± 0.43	0.93 ± 0.46	Khan et al. (2019)
Beijing, China	2005–2009	0.56–1.58	0.9–1.2	Wang et al. (2011)
Wuhan, China	2007–2013	1.05 ± 0.66	1.22	Wang et al. (2015)

photometers reported similar aerosol loading of 0.128 ± 0.003 (Sizov et al., 2015). Semenov et al. (2005) reported lower AOD based on observations during 2000–2004, indicating increment in aerosol loading during recent period. Aerosol loading over Issyk-Kul was similar to that observed over background sites like Muztagh Ata in eastern Pamirs (Yan et al., 2015) and Mt. Waliguan, a baseline Global Atmospheric Watch site located in northeastern part of the Tibetan Plateau, China (Che et al., 2011) whereas half of that in Dushanbe, a nearby capital city of Tajikistan (Rupakheti et al., 2020) and Zanjan, Iran (Bayat et al., 2011). Nevertheless, AOD in Issyk-Kul was more than twice higher than the remote sites like Nam Co and QOMS in the Tibetan Plateau (Pokharel et al., 2019). Regarding AE, the values were higher than over many sites listed in Table 1, indicating the dominance of fine aerosols over the Issyk-Kul site. Interestingly, the average AE value has not changed much compared to another study conducted over the same site (using Microtops sunphotometer) in the early 2000s (Semenov et al., 2005) which may indicate that the aerosol source has not changed much over the course of time.

Seasonal and monthly average aerosol parameters were also investigated using the daily mean data. In winter, mean AOD and AE were 0.12 ± 0.06 and 1.39 ± 0.32, respectively, with a FMF value of 0.79 ± 0.15, clearly indicating the dominance of fine aerosol in the atmosphere. Spring season observed the highest seasonal mean AOD (0.17 ± 0.17), lowest AE (0.91 ± 0.43), and lowest FMF (0.54 ± 0.20), indicating the presence of coarser particles in the atmosphere (contributing 59% to total AOD) than other seasons. During the other two seasons, AOD, AE and FMF were 0.13 ± 0.07, 1.27 ± 0.36 and 0.67 ± 0.16 (during summer) and 0.12 ± 0.08, 1.22 ± 0.38 and 0.69 ± 0.17 (during autumn), respectively. Month-wise mean (Fig. 3) AOD ranged between 0.10 ± 0.06 in December to 0.20 ± 0.23 in April. Similarly, monthly AE was in the range between 0.81 ± 0.45 (April) and 1.44 ± 0.32 (December). The columnar water vapor (CWV) ranged between 0.41 ± 0.14 cm (January) to 1.47 ± 0.24 cm (July). Monthly trend (figures not shown) of AOD (AE) exhibited very small increasing (decreasing) order with value of 3 × 10^{-6} (−4 × 10^{-5}) per month which were higher than as reported in Dushanbe, Tajikistan (Rupakheti et al., 2020). In Issyk-Kul, while considering total AOD, fine (coarse) mode exhibited decreasing (increasing) order with value of −2 × 10^{-6} (5 × 10^{-6}) per month. The highest monthly mean AOD in April, which is distinctly higher than other months, (with lowest AE) indicates the presence of coarse particles like dust in the atmosphere, which has been further supported by the lowest FMF (0.50 ± 0.21) during this month (~64% of total AOD was contributed by the coarse mode particles).

3.2. Aerosol types inferred from the relationship between AOD and AE

To the best of our knowledge, previous studies based on sunphotometer retrievals aerosol types have not been investigated over any background site in Central Asia. Different parameters from AERONET sunphotometer retrieved datasets can be utilized to analyze the aerosol types, the most commonly used method being an analysis of relation between AOD and AE (Kaskaoutis et al., 2007; Rupakheti et al., 2018; Sharma et al., 2014; Smirnov et al., 2002; Tiwari et al., 2018, 2016). Nevertheless, this method is unable to retrieve the aerosol types properties in the case of well-mixed aerosols and cannot further differentiate aerosols into absorbing and non-absorbing aerosols for which we need additional variables from AERONET dataset which is beyond the scope of this study. Previous studies have used threshold values of these two parameters for classification of various aerosol types as AOD <0.2 and AE >1.0 for clean continental, AOD <0.2 and AE <0.9 for clean marine, AOD >0.3 and AE >1.0 for urban/industrial and biomass burning, AOD >0.6 and AE <0.7 for dust, and that not falling within any these criteria is classified as the mixed aerosols over Central Asia ((Rupakheti et al., 2019, 2020; 2021). Over Issyk-Kul, the clean continental aerosol was dominant aerosol type (~65%), followed by mixed aerosols (~19%), and clean marine aerosols (~14%) (Fig. 4). The share of individual aerosol type is different than that observed over Dushanbe, where the highest share of mixed aerosol (57%), followed by clean continental (17%) and clean marine (15.7%) was observed (Rupakheti et al., 2020) which is understandable as Dushanbe is a capital city with significant anthropogenic activities whereas on the other hand, over Issyk-Kul, dust and aerosols from anthropogenic activities (urban and biomass burning) were less than 1% each.

The monthly and seasonal contribution of individual aerosol types is presented in Fig. 5. On a seasonal basis, clean continental aerosol type had the highest share over Issyk Kul, ~41% (spring) to ~81% (winter). In a previous study that utilized the satellite-retrieved data during 2002–2017, Rupakheti et al. (2019) reported that Kyrgyzstan has the highest share of clean continental aerosol (~90%) among five countries in Central Asia. The mixed aerosol type had the share of ~14%–~27% in Issyk-Kul (Fig. 4) which is formed either by an external or internal mixing of anthropogenic and natural aerosols (Pathak et al., 2012). The share of dust, which is more abundant during stormy seasons, was highest in the spring season (2.7%), followed by summer (0.5%) and autumn (~0.12%) and was absent in the winter season.

3.3. Aerosol volume concentration and volume size distribution

Fig. 6 shows the seasonal aerosol volume size distribution (VSD) derived from the sunphotometer measurements using 22 radius size bins ranging from 0.05 to 15 μm. It has a bi-modal distribution which can be defined by the sum of two log-normal distributions (Dubovik and King, 2000), as governed by the equation below:

$$v(r) = \frac{dV(r)}{d\ln r} = \sum_{i=1}^{2} \frac{C_{v,i}}{\sqrt{2\pi}\sigma_i} \exp\left[\frac{-(\ln r - \ln r_{v,i})}{2\sigma_i^2}\right]$$

Aerosol volume size distribution is bi-modal in every season with

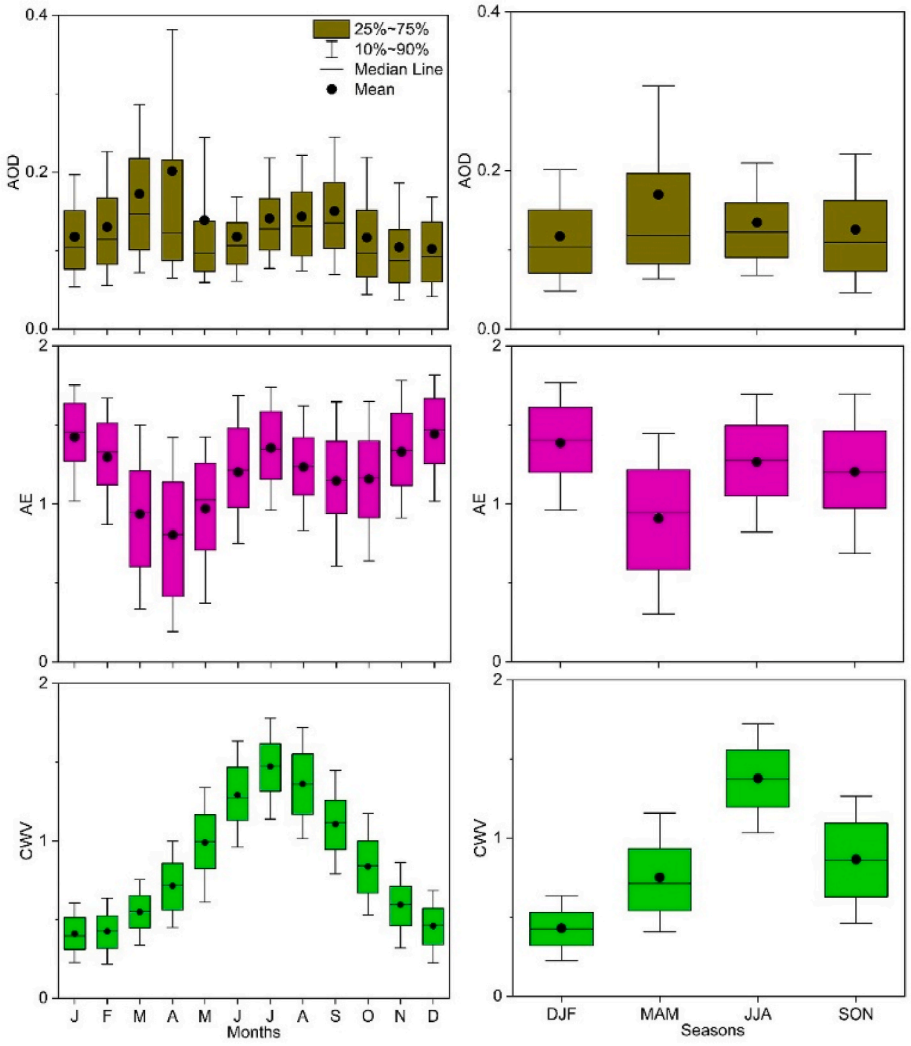

Fig. 3. Monthly and seasonal mean AOD, AE and columnar water vapor (CWV). In each box, the lower and upper boundary represent the 25th and 75th percentile, the top and bottom of the whisker represent the 90th and 10th percentile, the mid-line represents the median; and the filled circle represents the mean value. Abbreviations of each month starting from January and ending at December has been used.

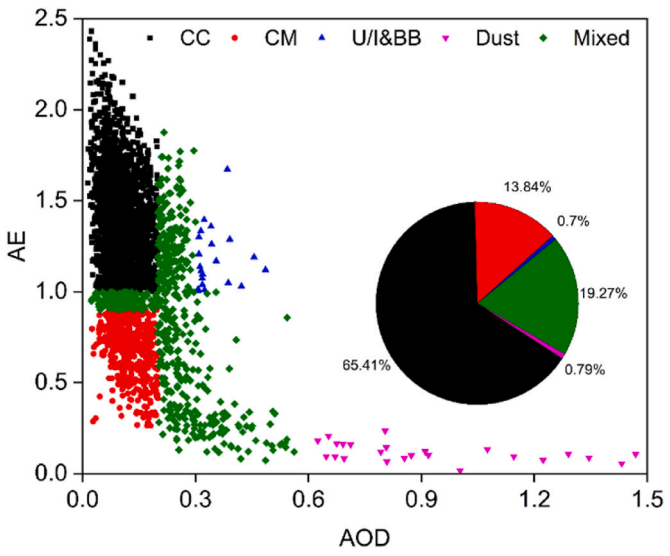

Fig. 4. Relation between AE and AOD used to estimate contributions of different aerosol types over Issyk-Kul. CC, CM and U/I & BB refer to clean continental, clean marine and urban/industrial & biomass burning aerosols.

modal radii at 0.1–0.15 μm (fine-mode) and 2–4 μm (coarse-mode), which indicates the influence of both anthropogenic (fine-mode with diameter ≤0.6 μm, such as those from fuel combustion) and natural (coarse-mode with diameter ≥0.6 μm, such as wind-blown dust) aerosols. Earlier studies have reported the fine (coarse) modal peak at radius 0.09–0.11 (1.71–3.86) μm at Dushanbe (Rupakheti et al., 2020), 0.2 (0.3) μm at Muztagh Ata (Yan et al., 2015), 0.2–0.3 (5) μm at Nam Co (Cong et al., 2009), 0.09–0.25 (2.2–2.9) μm, and 0.11–0.25 (2.2–3.8) μm during dust and haze-fog in Beijing (Yu et al., 2011), 0.11–0.19 (2.2–3.8) μm in Lanzhou, China (Yu et al., 2009). The shift in fine and coarse mode peak during the summer could be attributed to the high moisture availability in the atmosphere (Fig. 3) that leads the hygroscopic growth of aerosols. Higher values in the coarse mode in both volume concentrations and VSD during the spring season (in particular, in the month of April) reflect the influence of natural aerosols like dust. The coarse mode dominated the fine mode except in winter, as evident in the lower fine-mode fraction contributing to volume concentrations (Fig. 6b) and VSD (Fig. 6a).

Seasonal mean aerosol VSD parameters are presented in Table 2, which clearly show the coarse-mode volume concentration (V_c) higher by a factor of ~0.8–4.1 than in fine mode (V_f) (lowest during winter and highest during the spring). The V_c/V_f ratio has been reported to be as high as 50 in the dust from the western part of Africa and the Arabian

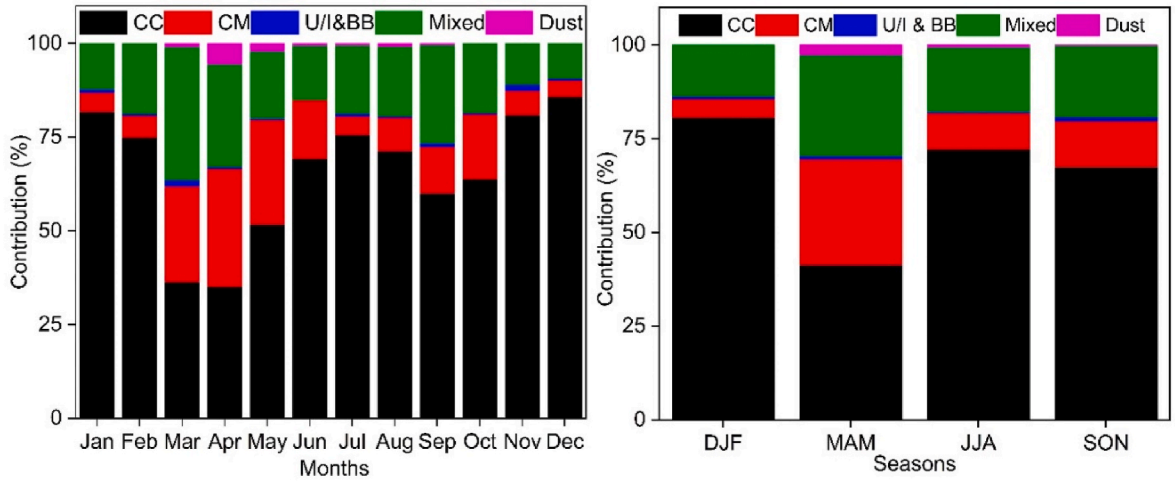

Fig. 5. Contributions of different types of aerosols in (a) monthly and (b) seasonal scale. CC, CM and U/I & BB refer to clean continental, clean marine and urban/industrial & biomass burning aerosols.

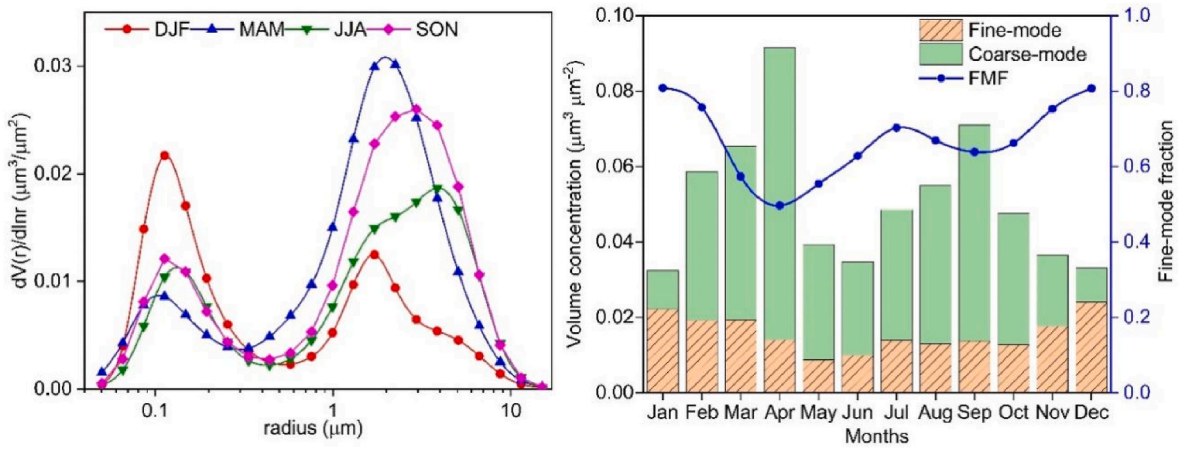

Fig. 6. Seasonal aerosol volume size distribution (left) and monthly aerosol volume concentration (right). DJF, MAM, JJA, and SON represent December–February (winter), March–May (spring), June–August (summer), and September–November (autumn), respectively.

Table 2
Seasonal mean parameters of aerosol volume size distribution over Issyk-Kul. V is the volume concentration ($\mu m^{-3}\mu m^{-2}$) for fine (f) and coarse (c) mode aerosols, R_{eff} is the effective radius (μm), VMR is the volume median radius (μm) and σ is its geometric standard deviation.

Seasons	V_f	R_{eff-f}	VMR_f	σ_f	V_c	R_{eff-c}	VMR_c	σ_c
DJF	0.022	0.131	0.145	0.474	0.017	2.170	2.646	0.632
MAM	0.012	0.132	0.150	0.523	0.049	1.529	1.952	0.700
JJA	0.012	0.137	0.151	0.442	0.035	2.169	2.769	0.681
SON	0.014	0.134	0.149	0.470	0.046	2.233	2.765	0.638

Peninsula, and ~10 in aerosols from the Bahrain-Persian Gulf (Dubovik et al., 2002), up to 8 during different seasons in Dushanbe (Rupakheti et al., 2020), and 6, 12, and 16 during the strong anthropogenic aerosol events, strong dust events, and extreme dust events over Dushanbe site in central Asia (Rupakheti et al., 2021). The effective radius of the fine mode (R_{eff-f}) was almost the same for all seasons (ca. 0.13 μm), whereas the effective radius of the coarse mode (R_{eff-c}) followed an order autumn (2.23) > winter (2.17) > spring (2.17) > spring (1.53). Such a behavior of minimal or no significant changes in the R_{eff-f} as compared to the R_{eff-c} could have a higher optical effect of aerosols (mostly in scattering efficiency) (Tiwari et al., 2015).

3.4. Characterization of high aerosol events

This section deals with the identification and investigation of aerosol properties on the high aerosol loading days during the measurement period. To identify the high aerosol episodes, we used the thresholds used earlier in other sites in central Asia (Hofer et al., 2017; Rupakheti et al., 2021) and other regions (Gkikas et al., 2013, 2016). If the AOD during any day was ≥average AOD over the observation period+(2 standard deviations), this was referred to as strong aerosol event day and if the average AOD was ≥average AOD+(4 standard deviations), it was considered as extreme aerosol event days. For our site, we found that 56 days observed AOD higher than 0.35 (strong event days) with mean AOD of 0.42 ± 0.06, and 25 days observed AOD higher than 0.56 (extreme event days) with mean AOD of 0.91 ± 0.26. Similarly, mean

AE (FMF) for these two types of events were found as 0.39 ± 0.36 (0.31 ± 0.18) and 0.12 ± 0.05 (0.19 ± 0.02), respectively, indicating the dominant presence of coarse particles (like dust) during the events. Exploring all events individually is out of the scope of this study. Thus, we collectively categorized the event days into strong and extreme events.

In Fig. 7, the relationship between AOD and AE (using threshold values mentioned in the earlier section) shows different types of aerosols during two types of events. Most of the aerosols during strong events were mixed and few urban/industrial and biomass burning. During the heavy aerosol events, 24 out of 25 days observed dust as indicated by low AE and high AOD. Similar to an earlier study (Rupakheti et al., 2021), this study also showed that the highest aerosol loading over central Asian sites is mostly dust-related.

The VSD during both type of events is also shown in Fig. 7, where one can observe the dominance of coarse mode. As the level 2 data for all days were not available, we opted to use the level 1.5 (cloud-screened) data for the VSD in this section. Unfortunately, the VSD data for some days with strong aerosol events (mainly resulting from anthropogenic activities as suggested by high AE values) could not be retrieved; otherwise, it would have been an excellent study to compare the natural and anthropogenic activities led event days in central Asian background site. The coarse mode modal radius was 1.70 μm during strong events and 2.24 μm during extreme events. During the whole observation period (all data), the modal radius in the coarse mode was observed at 2.24 μm. During the aerosol event days, the coarse mode aerosol volume concentration was higher by a factor of ~7.5 and ~19 compared to the average for the whole study period. Over Dushanbe in Central Asia, the maxima peaks observed at the same radius (2.2 μm) were higher by a factor of ~14 compared to the 2010–2018 period (Rupakheti et al., 2021). Similar types of enhancement in the coarse mode radius were reported in earlier studies over Kanpur (Prasad & Singh, 2007; Tiwari et al., 2019), Lahore (Alam et al., 2014), central Himalayas (Singh et al., 2022), Beijing (Yu et al., 2016) and Dushanbe (Rupakheti et al., 2021) during dust events.

3.5. Aerosol transport pathways

We analyzed the air mass back trajectories to understand the potential sources and transport pathways of aerosols only during December 2016–November 2017 as an example. Five-days long back trajectories of the air mass arriving at the height of 500 m agl over the Issyk-Kul site were calculated using the Hybrid Single-Particle Lagrangian Integrated Trajectory (HYSPLIT) model developed by the Air Resources Laboratory of the National Oceanic and Atmospheric Administration (NOAA) (www.arl.noaa.gov/HYSPLIT_ info. php) (Draxler and Hess, 1998; Stein et al., 2015) with 1 × 1° meteorological data retrieved from the Global Data Assimilation System (GDAS) (https://ready.arl.noaa.gov/gdas1.php).To effectively identify the potential source regions of aerosols, a widely used statistical tool in understanding the aerosol source region named potential source contribution function (PSCF) has been used (Tiwari et al., 2018; Yin et al., 2017, 2021; Hu et al., 2022; Rai et al., 2022). In this analysis, rain-bearing trajectories were sorted out in order to avoid the possible uncertainty (Cross, 2015) as done in another recent study (Rai et al., 2022). Afterwards, a Gaussian filter and continuous weighting function was used to smooth out the results:

$$WF_{ij} = \frac{\log(N_{ij})}{\log(\max(N))}$$

where WF_{ij} is the weighted function for N_{ij} trajectories and N represents the total number of trajectories.

Utilizing PSCF results, air mass associated with higher AOD during different seasons have been identified as shown in Fig. 8. As can be inferred from the figure, the contribution of AOD from within the Central Asian region is highest during all seasons with major contribution from local or regional sources. During all seasons, a significant influence of westerlies was also observed. During winter season, majority of aerosol were from within Kyrgyzstan, indicating the transport of local/regional aerosols to the site. Over Dushanbe, neighboring country Tajikistan's capital city, Rupakheti et al. (2020) reported 40–50% of the local/regional airmasses with the highest contribution (~53%) during the winter season. In summer, the contribution of aerosols (beside local origin) from neighboring country Kazakhstan's largest city and former capital city Almaty was observed. During spring, aerosols were contributed by the dust belt region, associated with the transport of coarse aerosols. Considerable fraction of AOD was contributed from four central Asian countries viz., Kyrgyzstan, Tajikistan, up to central Uzbekistan and western Turkmenistan during the autumn season. The origin and passing of air masses over the different types of land use/land cover regions might have resulted in transport of various types of aerosols observed over the Issyk-Kul region. Nevertheless, future studies are required to understand the aerosol chemistry (including isotopic analysis) and computer-based modelling works to properly apportion contributions of various aerosol sources and source regions.

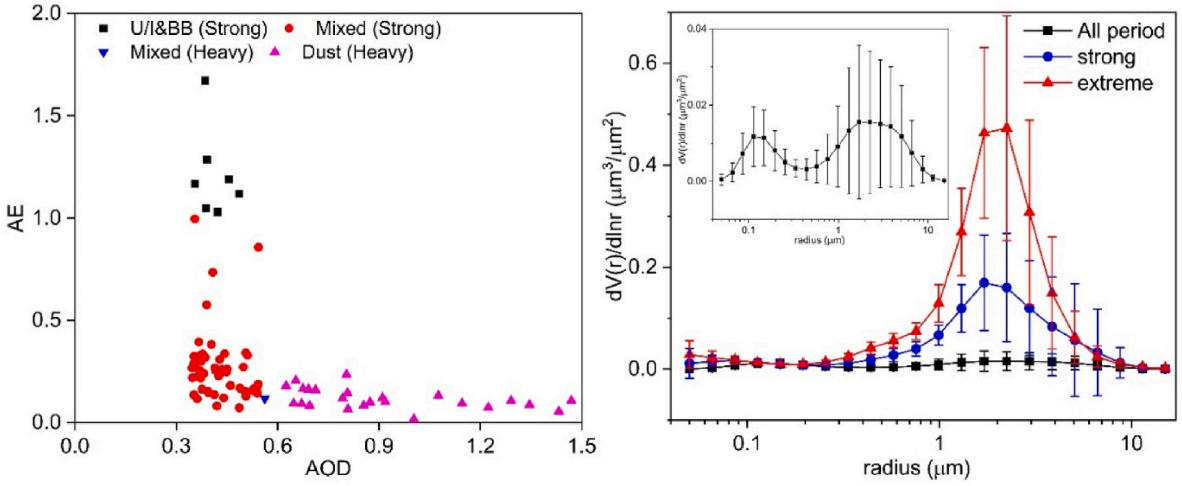

Fig. 7. Relationship between AOD and AE during two types of events (left) and aerosol volume size distribution (right). Inset in the right panel shows the VSD during all period.

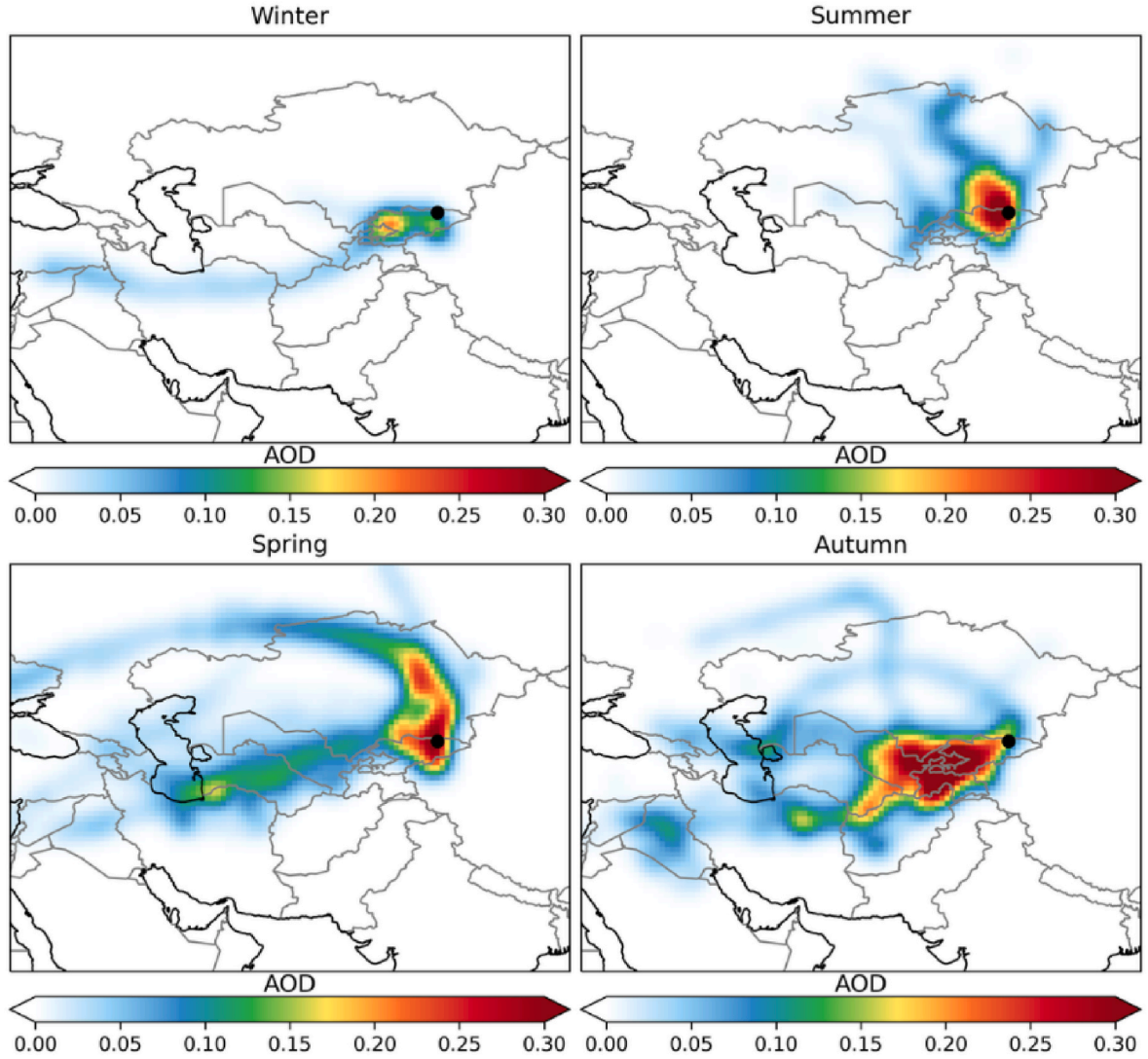

Fig. 8. Seasonal average Potential Source Contribution Analysis (PSCF) plots of 5 days air mass back trajectories at Issyk-Kul during different seasons over an observation period from December 2016 to November 2017.

4. Conclusions

This study was conducted to understand the columnar aerosol properties over a background site (Issyk-Kul Lake, Kyrgyzstan) in Central Asia. Using the data collected during 2007–2021, this study found the mean AOD of 0.14 ± 0.10 with the highest AOD (and lowest AE) during the spring season, indicating higher amounts of coarse aerosol in the atmosphere in spring. Aerosol types were classified based on a common methodology which showed the highest contribution of clean continental aerosols (~65%) followed by mixed aerosols (~19%) and clean marine aerosols (~14%). The contribution of dust was observed to be ~0.8% in total, with the highest contribution during spring followed by the summer season. These results are evidence of the presence of an 'aerosol cocktail' over this background site throughout the year with contributions of individual aerosol types varying across the seasons. The presence and influence of coarse mode aerosols on both aerosol loading and modifications of aerosol optical properties were observed during the heavy aerosol episodes as evident in the enhancement in the coarse mode aerosol volume by a factor of up to ~20 times higher (as compared to the whole observation period). The local and regional emissions from within the central Asia region was dominant source aerosols to Issyk-Kul site. As the central Asian region still observes the scantiness of research on aerosol properties and potential impacts, this study will aid scientists interested in the air quality and climate over this vast landmass. Future studies should be designed using state of the art instruments for observation of aerosol physical and chemical properties, both surface and columnar, and sophisticated computer models with appropriate representation of emissions and meteorology of the region to understand air pollution, its origin, proportional contributions of various sources and regions, and its effects over this region and downwind regions.

Credit author statement

Dipesh Rupakheti: Conceptualization, Formal analysis, Visualization, Writing-original draft. **Maheswar Rupakheti**: Conceptualization, Writing-review & editing. **Mukesh Rai**: Visualization, Writing-review & editing. **Xingna Yu**: Writing-review & editing. **Xiufeng Yin**: Writing-review & editing. **Shichang Kang**: Writing-review & editing. **Musapar D. Orozaliev**: Resources, Writing-review & editing. **Valery P. Sinyakov**: Resources, Writing-review & editing. **Sabur F. Abdullaev**: Writing-review & editing. **Ishaq D imeji Sulaymon**: Writing-review & editing. **Jianlin Hu**: Writing-review & editing.

Declaration of competing interest

The authors declare that they have no known competing financial

interests or personal relationships that could have appeared to influence the work reported in this paper.

Data availability

Freely available data from the AERONET website (https://aeronet.gsfc.nasa.gov/) has been used in this study.

Acknowledgments

This work was supported by the National Natural Science Foundation of China (41975162, 42021004). Dipesh Rupakheti acknowledges The Startup Foundation for Introducing Talent of NUIST (2022r024). Maheswar Rupakheti acknowledges the support provided by the Institute for Advanced Sustainability Studies (IASS), which is funded by the German Federal Ministry for Education and Research (BMBF) and the Brandenburg Ministry for Science, Research, and Culture (MWFK). All authors are grateful to Brent Holben (NASA GSFC, USA) for establishing the AERONET site at Issyk-Kul, and Prof. Phillipe Goloub and staffs for their efforts for the annual calibration of the sunphotometer.

References

Alam, K., Trautmann, T., Blaschke, T., Subhan, F., 2014. Changes in aerosol optical properties due to dust storms in the Middle East and Southwest Asia. Remote Sens. Environ. 143, 216–227.

Bayat, A., Masoumi, A., Khalesifard, H.R., 2011. Retrieval of atmospheric optical parameters from ground-based sun-photometer measurements for Zanjan, Iran. Atmos. Meas. Tech. 4, 857–863.

Burney, J., Ramanathan, V., 2014. Recent climate and air pollution impacts on Indian agriculture. Proc. Natl. Acad. Sci. U. S. A 111, 16319–16324.

Chameides, W.L., Yu, H., Liu, S.C., Bergin, M., Zhou, X., Mearns, L., Wang, G., Kiang, C. S., Saylor, R.D., Luo, C., Huang, Y., 1999. Case study of the effects of atmospheric aerosols and regional haze on agriculture an opportunity to enhance crop yields in China through emission controls? Proc. Natl. Acad. Sci. USA 96, 13626–13633.

Che, H., Wang, Y., Sun, J., 2011. Aerosol optical properties at Mt. Waliguan observatory, China. Atmos. Environ. 45 (33), 6004–6009.

Chen, B.B., Sverdlik, L.G., Imashev, S.A., Solomon, P.A., Lantz, J., Schauer, J.J., Shafer, M.M., Artamonova, M.S., Carmichael, G.R., 2013a. Lidar measurements of the vertical distribution of aerosol optical and physical properties over central Asia. Int. J. Atmos. Sci. 1–17, 2013.

Chen, B.B., Sverdlik, L.G., Imashev, S.A., Solomon, P.A., Lantz, J., Schauer, J.J., Shafer, M.M., Artamonova, M.S., Carmichael, G., 2013b. Empirical relationship between particulate matter and aerosol optical depth over Northern Tien-Shan, Central Asia. Air Qual. Atmos. Health 6 (2), 385–396.

Chen, B.B., Imashev, S.A., Sverdlik, L.G., Solomon, P.A., Lantz, J., Schauer, J.J., Shafer, M.M., Artamonova, M.S., Carmichael, G.R., 2013. Ozone variations over central Tien-Shan in Central Asia and implications for regional emissions reduction strategies. Aerosol Air Qual. Res. 13 (2), 555–562.

Cohen, A.J., Brauer, M., Burnett, R., Anderson, H.R., Frostad, J., Estep, K., Balakrishnan, K., Brunekreef, B., Dandona, L., Dandona, R., Feigin, V., Freedman, G., Hubbell, B., Jobling, A., Kan, H., Knibbs, L., Liu, Y., Martin, R., Morawska, L., Pope, C.A., Shin, H., Straif, K., Shaddick, G., Thomas, M., van Dingenen, R., van Donkelaar, A., Vos, T., Murray, C.J.L., Forouzanfar, M.H., 2017. Estimates and 25-year trends of the global burden of disease attributable to ambient air pollution: an analysis of data from the Global Burden of Diseases Study 2015. Lancet 389, 1907–1918.

Cong, Z., Kang, S., Smirnov, A., Holben, B., 2009. Aerosol optical properties at Nam Co, a remote site in central Tibetan Plateau. Atmos. Res. 92, 42–48.

Cross, M., 2015. PySPLIT: a package for the generation, analysis, and visualizations of HYSPLIT air parcel trajectories. In: Paper Presented at Proceedings of 14th Annual Scientific Computing with Python Conference (SciPy 15).

Dewan, N., Majestic, B.J., Ketterer, M.E., Miller-Schulze, J.P., Shafer, M.M., Schauer, J.J., Solomon, P.A., Artamonova, M., Chen, B.B., Imashev, S.A., Carmichael, G.R., 2015. Stable isotopes of lead and strontium as tracers of sources of airborne particulate matter in Kyrgyzstan. Atmos. Environ. 120, 438–446.

Draxler, R.R., Hess, G.D., 1998. An overview of the HYSPLIT_4 modelling system for trajectories, dispersion, and deposition. Aust. Meteorol. Mag. 47, 295–308.

Dubovik, O., King, M.D., 2000. A flexible inversion algorithm for retrieval of aerosol optical properties from Sun and sky radiance measurements. J. Geophys. Res. 105, 20673–20696.

Dubovik, O., Kaufman, Y.J., King, M.D., Eck, T.F., Smirnov, A., Tanr e, D., Holben, B., Slutsker, I., 2002. Variability of absorption and optical properties of key aerosol types observed in worldwide locations. J. Atmos. Sci. 59, 590–608.

Dubovik, O., Smirnov, A., Holben, B.N., King, M.D., Kaufman, Y.J., Eck, T.F., Slutsker, I., 2000. Accuracy assessments of aerosol optical properties retrieved from Aerosol Robotic Network (AERONET) Sun and sky radiance measurements. J. Geophys. Res. Atmos. 105 (D8), 9791–9806.

Giles, D.M., Sinyuk, A., Sorokin, M.S., Schafer, J.S., Smirnov, A., Slutsker, I., Eck, T.F., Holben, B.N., Lewis, J., Campbell, J., Welton, E.J., Korkin, S., Lyapustin, A., 2019. Advancements in the aerosol robotic network (AERONET) version 3 database – automated near real-time quality control algorithm with improved cloud screening for sun photometer aerosol optical depth (AOD) measurements. Atmos. Meas. Tech. 12, 169–209.

Gkikas, A., Basart, S., Hatzianastassiou, N., Marinou, E., Amiridis, V., Kazadzis, S., Pey, J., Querol, X., Jorba, O., Gassó, S., Baldasano, J.M., 2016. Mediterranean intense desert dust outbreaks and their vertical structure based on remote sensing data. Atmos. Chem. Phys. 16, 8609–8642.

Gkikas, A., Hatzianastassiou, N., Mihalopoulos, N., Katsoulis, V., Kazadzis, S., Pey, J., Querol, X., Torres, O., 2013. The regime of intense desert dust episodes in the Mediterranean based on contemporary satellite observations and ground measurements. Atmos. Chem. Phys. 13, 12135–12154.

Golitsyn, G., Gillette, D.A., 1993. Introduction: a joint Soviet-American experiment for the study of Asian desert dust and its impact on local meteorological conditions and climate. Atmos. Environ. 27A, 2467–2470.

Hofer, J., Althausen, D., Abdullaev, S.F., Makhmudov, A.N., Nazarov, B.I., Schettler, G., Engelmann, R., Baars, H., Fomba, K.W., Müller, K., Heinold, B., Kandler, K., Ansmann, A., 2017. Long-term profiling of mineral dust and pollution aerosol with multiwavelength polarization Raman lidar at the Central Asian site of Dushanbe, Tajikistan: case studies. Atmos. Chem. Phys. 17, 14559–14577.

Holben, B.N., Eck, T.F., Slutsker, I., Tanre, D., Buis, J.P., Setzer, A., Vermote, E., Reagan, J.A., Kaufman, Y.J., Nakajima, T., Lavenu, F., Jankowiak, I., Smirnov, A., 1998. Aeronet - a federated instrument network and data archive for aerosol characterization. Remote Sens. Environ. 66, 1–16.

Holben, B.N., Tanré, D., Smirnov, A., Eck, T.F., Slutsker, I., Abuhassan, N., Newcomb, W. W., Schafer, J.S., Chatenet, B., Lavenu, F., Kaufman, Y.J., Vande Castle, J., Setzer, A., Markham, B., Clark, D., Frouin, R., Halthore, R., Karneli, A., O'Neill, N.T., Pietras, C., Pinker, R.T., Voss, K., Zibordi, G., Tanre, D., Smirnov, A., Eck, T.F., Slutsker, I., Abuhassan, N., Newcomb, W.W., Schafer, J.S., Chatenet, B., Lavenu, F., Kaufman, Y.J., Castle, J.V., Setzer, A., Markham, B., Clark, D., Frouin, R., Halthore, R., Karneli, A., O'Neill, N.T., Pietras, C., Pinker, R.T., Voss, K., Zibordi, G., 2001a. An emerging ground-based aerosol climatology: aerosol optical depth from AERONET. J. Geophys. Res. 106, 12067–12097.

Holben, B.N., Tanre, D., Smirnov, A., Eck, T.F., Slutsker, I., Abuhassan, N., et al., 2001b. An emerging ground-based aerosol climatology: aerosol optical depth from AERONET. J. Geophys. Res. Atmos. 106 (D11), 12067–12097.

Hu, J., Huang, L., Chen, M., Liao, H., Zhang, H., Wang, S., et al., 2017. Premature mortality attributable to particulate matter in China: source contributions and responses to reductions. Environ. Sci. Technol. 51 (17), 9950–9959.

Hu, Y., Kang, S., Yang, J., Ji, Z., Rupakheti, D., Yin, X., Du, H., 2022. Impact of atmospheric circulation patterns on properties and regional transport pathways of aerosols over Central-West Asia: emphasizing the Tibetan Plateau. Atmos. Res. 266, 105975.

IPCC, 2021. Climate Change 2021: the Physical Science Basis. Contribution of Working Group I to the Sixth Assessment Report of the Intergovernmental Panel on Climate Change. Cambridge University Press, Cambridge, United Kingdom and New York, NY, USA.

Immerzeel, W.W., van Beek, L.P.H., Bierkens, M.F.P., 2010. Climate change will affect the Asian water towers. Science 328, 1382–1385.

Kampa, M., Castanas, E., 2008. Human health effects of air pollution. Environ. Pollut. 151, 362–367.

Kang, S., Zhang, Q., Qian, Y., Ji, Z., Li, C., Cong, Z., Zhang, Y., Guo, J., Du, W., Huang, J., You, Q., Panday, A.K., Rupakheti, M., Chen, D., Gustafsson, O., Thiemens, M.H., Qin, D., 2019. Linking atmospheric pollution to cryospheric change in the Third Pole region: current progress and future prospects. Natl. Sci. Rev. 6, 796–809.

Kaskaoutis, D.G., Kambezidis, H.D., Hatzianastassiou, N., Kosmopoulos, P.G., Badarinath, K.V.S., 2007. Aerosol climatology: on the discrimination of aerosol types over four AERONET sites. Atmos. Chem. Phys. Discuss. 7, 6357–6411.

Kaufman, Y.J., Tanré, D., Boucher, O., 2002. A satellite view of aerosols in the climate system. Nature 419, 215–223.

Khan, R., Kumar, K.R., Zhao, T., 2019. The climatology of aerosol optical thickness and radiative effects in Southeast Asia from 18-years of ground-based observations. Environ. Pollut. 254, 113025.

Li, Q., Wu, J., Zhou, J., et al., 2020. Occurrence of polycyclic aromatic hydrocarbon (PAH) in soils around two typical lakes in the western Tian Shan Mountains (Kyrgyzstan, Central Asia): local burden or global distillation? Ecol. Indicat. 108, 105749.

Liu, T., Wang, X., Hu, J., Wang, Q., An, J., Gong, K., et al., 2020. Driving forces of changes in air quality during the COVID-19 lockdown period in the Yangtze River Delta Region, China. Environ. Sci. Technol. Lett. 7 (11), 779–786.

Liu, Y., Zhu, Q., Wang, R., Xiao, K., Cha, P., 2019. Distribution, source and transport of the aerosols over Central Asia. Atmos. Environ. 210, 120–131.

Pathak, B., Bhuyan, P.K., Gogoi, M., Bhuyan, K., 2012. Seasonal heterogeneity in aerosol types over Dibrugarh-North-Eastern India. Atmos. Environ. 47, 307–315.

Pokharel, M., Guang, J., Liu, B., Kang, S., Ma, Y., Holben, B.N., Xia, X., Xin, J., Ram, K., Rupakheti, D., Wan, X., Wu, G., Bhattarai, H., Zhao, C., Cong, Z., 2019. Aerosol properties over Tibetan Plateau from a decade of AERONET measurements: baseline, types, and influencing factors. J. Geophys. Res. Atmos. 124 (23), 13357–13374.

Prasad, A.K., Singh, R.P., 2007. Comparison of MISR-MODIS aerosol optical depth over the Indo-Gangetic basin during the winter and summer seasons (2000– 2005). Remote Sens. Environ. 107, 109–119.

Prospero, J.M., Ginoux, P., Torres, O., Nicholson, S.E., Gill, T.E., 2002. Environmental characterization of global sources of atmospheric soil dust identified with the

Nimbus 7 Total Ozone Mapping Spectrometer (TOMS) absorbing aerosol product. Rev. Geophys. 40 (1), 2-1-2-23.
Rai, M., Kang, S., Yang, J., Chen, X., Hu, Y., Rupakheti, D., 2022. Tracing atmospheric anthropogenic Black carbon and its potential radiative response over pan-third Pole region: a synoptic-scale Analysis using WRF-chem. J. Geophys. Res. Atmos. 127 (6), e2021JD035772.
Ramachandran, S., Rupakheti, M., 2022. Trends in physical, optical and chemical columnar aerosol characteristics and radiative effects over South and East Asia: satellite and ground-based observations. Gondwana Res. 105, 366–387.
Ramanathan, V., Crutzen, P.J., Kiehl, J.T., Rosenfeld, D., 2001. Aerosols, climate, and the hydrological cycle. Science 80 (294), 2119–2125.
Ramanathan, V., Li, F., Ramana, M.V., Praveen, P.S., Kim, D., Corrigan, C.E., Nguyen, H., Stone, E.A., Schauer, J.J., Carmichael, G.R., Adhikary, B., Yoon, S.C., 2007. Atmospheric brown clouds: hemispherical and regional variations in long-range transport,absorption, and radiative forcing. J. Geophys. Res. 112, 1–26.
Rosenfeld, D., 2000. Suppression of rain and snow by urban and industrial air pollution. Science 287 (5459), 1793–1796.
Rupakheti, D., Kang, S., Rupakheti, M., Chen, P., Gautam, S., Rai, M., Yin, X., Kang, H., 2021. Black carbon in surface soil and its sources in three central Asian countries. Arch. Environ. Contam. Toxicol. 80 (3), 558–566.
Rupakheti, D., Rupakheti, M., Abdullaev, S.F., Yin, X., Kang, S., 2020. Columnar aerosol properties and radiative effects over Dushanbe, Tajikistan in Central Asia. Environ. Pollut. 265, 1–12.
Rupakheti, D., Kang, S., Bilal, M., Gong, J., Xia, X., Cong, Z., 2019. Aerosol optical depth climatology over Central Asian countries based on Aqua-MODIS Collection 6.1 data: aerosol variations and sources. Atmos. Environ. 207, 205–214.
Rupakheti, D., Kang, S., Rupakheti, M., Cong, Z., Tripathee, L., Panday, A.K., Holben, B. N., 2018. Observation of optical properties and sources of aerosols at Buddha's birthplace, Lumbini, Nepal: environmental implications. Environ. Sci. Pollut. Control Ser. 25 (15), 14868–14881.
Sayer, A.M., Hsu, N.C., Bettenhausen, C., Jeong, M.J., Holben, B.N., Zhang, J., 2012. Global and regional evaluation of over-land spectral aerosol optical depth retrievals from SeaWiFS. Atmos. Meas. Tech. 5 (7), 1761–1778.
Schuster, G.L., Dubovik, O., Holben, B.N., 2006. Ångström exponent and bimodal aerosol size distributions. J. Geophys. Res. 111, D07207.
Semenov, V.K., Smirnov, A., Aref'ev, V.N., Sinyakov, V.P., Sorokina, L.I., Ignatova, N.I., 2005. Aerosol optical depth over the mountainous region in central Asia (Issyk-Kul Lake, Kyrgyzstan). Geophys. Res. Lett. 32 (5), L05807.
Sharma, M., Kaskaoutis, D.G., Singh, R.P., Singh, S., 2014. Seasonal variability of atmospheric aerosol parameters over greater Noida using ground sunphotometer observations. Aerosol Air Qual. Res. 14, 608–622.
Sierra-Hernández, M.R., Beaudon, E., Gabrielli, P., Thompson, L., 2019. 21st-century Asian air pollution impacts glacier in northwestern Tibet. Atmos. Chem. Phys. 19 (24), 15533–15544.
Singh, J., Singh, N., Ojha, N., Srivastava, A.K., Bisht, D.S., Rajeev, K., Kumar, K.N., Singh, R.S., Panwar, V., Dhaka, S.K., Kumar, V., 2022. Genesis of a severe dust storm over the Indian subcontinent: dynamics and impacts. Earth Space Sci. 9 (2) e2021EA001702.
Sinyuk, A., Holben, B.N., Eck, T.F., Giles, D.M., Slutsker, I., Korkin, S., et al., 2020. The AERONET Version 3 aerosol retrieval algorithm, associated uncertainties and comparisons to Version 2. Atmos. Meas. Tech. 13 (6), 3375–3411.
Sizov, N.I., Akimenko, R.M., Aref'ev, V.N., Kashin, F.V., Orozaliev, M.D., Sinyakov, V.P., Sorokina, L.I., 2015. Variability of atmospheric aerosol optical depth over the Northern Tian Shan. Russ. Meteorol. Hydrol. 40 (3), 180–185.
Smirnov, A., Holben, B.N., Eck, T.F., Dubovik, O., Slutsker, I., 2000. Cloud-screening and quality control algorithms for the AERONET database. Remote Sens. Environ. 73, 337–349.
Smirnov, A., Holben, B.N., Dubovik, O., O'Neill, N.T., Eck, T.F., Westphal, D.L., Goroch, A.K., Pietras, C., Slutsker, I., 2002. Atmospheric aerosol optical properties in the Persian Gulf. J. Atmos. Sci. 59 (3), 620–634.
Srivastava, A.K., Tiwari, S., Devara, P.C.S., Bisht, D.S., Srivastava, M.K., Tripathi, S.N., Goloub, P., Holben, B.N., 2011. Pre-monsoon aerosol characteristics over the Indo-Gangetic Basin: implications to climatic impact. Ann. Geophys. 29, 789–804.
Stein, A.F., Draxler, R.R., Rolph, G.D., Stunder, B.J.B., Cohen, M.D., Ngan, F., 2015. NOAA's HYSPLIT atmospheric transport and dispersion modeling system. Bull. Am. Meteorol. Soc. 96, 2059–2077.
Stocker, T., Qin, D., Plattner, G., Tignor, M., Allen, S., Boschung, J., Nauels, A., Xia, Y., Bex, B., Midgley, B., 2013. IPCC, 2013: Climate Change 2013: the Physical Science Basis. Contribution of Working Group I to the Fifth Assessment Report of the Intergovernmental Panel on Climate Change.
Tiwari, S., Kumar, A., Pratap, V., Singh, A.K., 2019. Assessment of two intense dust storm characteristics over Indo – gangetic basin and their radiative impacts: a case study. Atmos. Res. 228, 23–40.
Tiwari, S., Dumka, U.C., Kaskaoutis, D.G., Ram, K., Panicker, A.S., Srivastava, M.K., Tiwari, Shani, Attri, S.D., Soni, V.K., Pandey, A.K., 2016. Aerosol chemical characterization and role of carbonaceous aerosol on radiative effect over Varanasi in central Indo-Gangetic Plain. Atmos. Environ. 125, 437–449.
Tiwari, S., Kaskaoutis, D., Soni, V.K., Dev Attri, S., Singh, A.K., 2018. Aerosol columnar characteristics and their heterogeneous nature over Varanasi, in the central Ganges valley. Environ. Sci. Pollut. Res. 25, 24726–24745.
Tiwari, S., Srivastava, A.K., Singh, A.K., Singh, S., 2015. Identification of aerosol types over Indo-Gangetic Basin: implications to optical properties and associated radiative forcing. Environ. Sci. Pollut. Res. 22, 12246–12260.
Wang, S., Fang, L., Gu, X., Yu, T., Gao, J., 2011. Comparison of aerosol optical properties from Beijing and Kanpur. Atmos. Environ. 45, 7406–7414.
Wang, L., Gong, W., Xia, X., Zhu, J., Li, J., Zhu, Z., 2015. Long-term observations of aerosol optical properties at Wuhan, an urban site in Central China. Atmos. Environ 101, 94–102.
Wang, C., Wang, Y., Shi, Z., Sun, J., Gong, K., Li, J., et al., 2021. Effects of using different exposure data to estimate changes in premature mortality attributable to PM2. 5 and O3 in China. Environ. Pollut. 285, 117242.
Xia, X., Chen, H., Wang, P., 2004. Aerosol properties in a Chinese semiarid region. Atmos. Environ. 38, 4571–4581.
Yan, N., Wu, G., Zhang, X., Zhang, C., Xu, T., 2015. Variation of aerosol optical properties from AERONET observation at Mt. Muztagh Ata, Eastern Pamirs. Atmos. Res. 153, 480–488.
Yin, X., Kang, S., de Foy, B., Rupakheti, D., Rupakheti, M., Cong, Z., et al., 2021. Impacts of Indian summer monsoon and stratospheric intrusion on air pollutants in the inland Tibetan Plateau. Geosci. Front. 12 (6), 101255.
Yin, X., Kang, S., de Foy, B., Cong, Z., Luo, J., Zhang, L., et al., 2017. Surface ozone at Nam Co in the inland Tibetan Plateau: variation, synthesis comparison and regional representativeness. Atmos. Chem. Phys. 17 (18), 11293–11311.
Yu, X., Lü, R., Kumar, K.R., Ma, J., Zhang, Q., Jiang, Y., Kang, N., Yang, S., Wang, J., Li, M., 2016. Dust aerosol properties and radiative forcing observed in spring during 2001–2014 over urban Beijing, China. Environ. Sci. Pollut. Res. 23, 15432–15442.
Yu, X., Zhu, B., Yin, Y., Yang, J., Li, Y., Bu, X., 2011. A comparative analysis of aerosol properties in dust and haze-fog days in a Chinese urban region. Atmos. Res. 99 (2), 241–247.
Yu, X., Bin, Z., Shuxian, F., Yan, Y., Xiaoli, B., 2009. Ground-based observation of aerosol optical properties in Lanzhou, China. J. Environ. Sci. 21 (11), 1519–1524.
Yu, Y., Pi, Y., Yu, X., Ta, Z., Sun, L., Disse, M., Zeng, F., Li, Y., Chen, X., Yu, R., 2019. Climate change, water resources and sustainable development in the arid and semi-arid lands of Central Asia in the past 30 years. J. Arid Land 11 (1), 1–14.